Cooperative orbital ordering and Peierls instability in the checkerboard lattice with doubly degenerate orbitals

R. T. Clay,[1] H. Li,[2] S. Sarkar,[3] S. Mazumdar,[2] and T. Saha-Dasgupta[3]
[1]*Department of Physics and Astronomy and HPC2 Center for Computational Sciences, Mississippi State University, Mississippi State, Mississippi 39762, USA*
[2]*Department of Physics, University of Arizona, Tucson, Arizona 85721, USA*
[3]*S. N. Bose National Centre for Basic Sciences, Kolkata, India*
(Received 11 March 2010; revised manuscript received 17 May 2010; published 13 July 2010)

It has been suggested that the metal-insulator transitions in a number of spinel materials with partially filled t_{2g} d orbitals can be explained as orbitally driven Peierls instabilities. Motivated by these suggestions, we examine theoretically the possibility of formation of such orbitally driven states within a simplified theoretical model, a two-dimensional checkerboard lattice with two-directional metal orbitals per atomic site. We include orbital ordering and interatom electron-phonon interactions self-consistently within a semiclassical approximation, and onsite intraorbital and interorbital electron-electron interactions at the Hartree-Fock level. We find a stable, orbitally induced Peierls bond-dimerized state for carrier concentration of one electron per atom. The Peierls bond distortion pattern continues to be period two bond dimerization even when the charge density in the orbitals forming the one-dimensional band is significantly smaller than 1. In contrast, for carrier density of half an electron per atom the Peierls instability is absent within one-electron theory as well as mean-field theory of electron-electron interactions, even for nearly complete orbital ordering. We discuss the implications of our results in relation to complex charge, bond, and orbital ordering found in spinels.

DOI: 10.1103/PhysRevB.82.035108 PACS number(s): 71.30.+h, 71.28.+d, 71.10.Fd

I. INTRODUCTION

Transition-metal spinel compounds AB_2X_4, where X is S or O, have been for many years the subject of intense experimental and theoretical activity. The B sublattice of the spinel structure forms corner-sharing tetrahedra, giving rise to a geometrically frustrated pyrochlore lattice. In general, oxides and chalcogenides of transition metals exhibit complex charge and spin ordering that are often coupled with orbital ordering.[1,2] Coupled orbital-charge-spin orderings have been investigated widely for compounds of the late transition metal ions with active e_g orbitals within cubic geometry, such as the cuprates and manganites. In contrast, such orderings in spinel compounds are only beginning to be studied.[3] Spinel systems are considerably more complicated than the cuprates or manganites due to two distinct reasons. First, the B ions in the spinels, which are in an octahedral environment of the X anions, often possess partially filled t_{2g} d orbitals. Examples include V^{3+} ions in the vanadates of Zn,[4,5] Mn,[6] and Cd;[7] $V^{2.5+}$ in AlV_2O_4;[8] Ti^{3+} in $MgTi_2O_4$;[9] $Ir^{3.5+}$ in $CuIr_2S_4$;[10] and $Rh^{3.5+}$ in $LiRh_2O_4$.[11] The threefold degeneracy of the t_{2g} orbitals, along with the weaker tendency to Jahn-Teller (JT) distortions[12] in t_{2g}-based systems lead to more complicated physics compared to e_g-based systems. Second, the geometric frustration in the spinel structure, mentioned above, precludes simple orderings.[3]

Very recently, an exotic orbitally induced Peierls instability has been proposed as the mechanism behind the metal-insulator transitions in the spinels such as $CuIr_2S_4$.[13] Charge segregation of Ir into formally Ir^{3+} and Ir^{4+}, accompanied by the formation of an octamer of Ir^{4+} ions with alternate short and long bonds is observed in $CuIr_2S_4$.[10] This unusual charge-ordering pattern has been explained within the context of an effective one-dimensionalization and Peierls instability driven by orbital ordering (OO). The spinel structure of $CuIr_2S_4$ consists of criss-cross chains of Ir ions with strongest overlaps between orbitals of the same kind (i.e., d_{xy} with d_{xy}, d_{yz} with d_{yz}). Within the proposed mechanism, OO in $Ir^{3.5+}$ ions leads to completely filled degenerate d_{xz} and d_{yz} orbitals and effective one-dimensional (1D) quarter-filled d_{xy} bands. The latter now undergoes a Peierls instability that is accompanied by period 4 charge ordering $\cdots Ir^{3+}/Ir^{3+}/Ir^{4+}/Ir^{4+}\cdots$ and long-intermediate-short-intermediate bonds, as seen experimentally.[10] The OO and Peierls instability are thought to be coupled, as opposed to independent. Closely related phenomenologies have been proposed to explain the metal-insulators transitions in $MgTi_2O_4$ (Ref. 13) and $LiRh_2O_4$.[11]

While the proposed scenario[13] does provide qualitative explanations, it raises many interesting questions. For example, the bond or charge periodicities that result from Peierls distortion in real quasi-1D systems depend strongly on the band filling. Naively then, one might be led to believe that unless the OO is complete and leads to integer occupations of the individual t_{2g} orbitals, exactly commensurate distortion periodicities, as supposedly observed in $CuIr_2S_4$ (Ref. 10) and $MgTi_2O_4$,[9] are not expected. The exactly period 4 distortion in $CuIr_2S_4$ and $MgTi_2O_4$ is therefore a puzzle. Second, the role of electron-electron (e-e) interactions, which can have important consequences on these transitions, is not clear. For example, it has been suggested that the bond distortion in $MgTi_2O_4$ causes nearest-neighbor Ti^{3+} pairs to form a spin-singlet state, giving a drop in the magnetic susceptibility at low temperature.[14] Furthermore, e-e interactions can strongly affect the distortion periodicities in 1D chains with fillings different from 1 electron per atom.[15] Addressing these issues requires explicit calculations based on Hamiltonians containing all the necessary

 ©2010 The American Physical Society

components, that to the best of our knowledge do not exist currently.

We report here the results of explicit calculations based on a simplified model system that displays cooperative OO and Peierls instability. Our model system is a two-dimensional projection of the pyrochlore lattice, a checkerboard lattice with two degenerate directional orbitals per atom. As we discuss in the next Section, the model captures the effective one-dimensionalization that occurs in the spinel lattice. There exist also subtle differences between the our model and the theoretical picture that has been employed for the spinels,[13] that we discuss in Sec. IV. We have considered two different electron densities, 1 electron per atom and $\frac{1}{2}$ electron per atom. We find that a stable Peierls state with 1D order occurs for an electron density of 1 electron per atom. Importantly, even for significant deviations of orbital occupancies from integer values, the Peierls distortion is purely bond dimerization, as would be true in the precisely $\frac{1}{2}$-filled 1D band. We speculate that this is a consequence of interactions between the effective 1D chains of our model, which are not entirely independent. For the case of $\frac{1}{2}$ electron per atom we did not observe an orbitally driven Peierls state even for integer orbital occupancies in the absence of e-e interactions. For the same model in the limit of infinite e-e interactions, however, a stable bond dimerization occurs. This suggests the second main result of our paper, namely, that e-e interactions are important in stabilizing orbitally induced Peierls states for the case of $\frac{1}{2}$ electron per atom within the orbitally degenerate checkerboard lattice. We will discuss possible implications of this result for the spinel lattice.

The paper is divided in following sections: in Sec. II we introduce our model Hamiltonian; in Secs. III A and III B we present numerical results for 1 and $\frac{1}{2}$ electron per atom, respectively; and in Sec. IV we conclude and further discuss the relationship of our theory to spinels and related materials.

II. THEORETICAL MODEL

As discussed above, no quantitative calculations exist of coexisting orbital and Peierls order in spinel lattices. This is due to the huge complexity of these systems, which include three dimensionality, triply degenerate t_{2g} metal atom orbitals, possible JT distortions and frustration, in addition to e-e interactions. We therefore construct a simpler model based on a checkerboard lattice that is easier to handle but that is expected to bear similarities with the spinel problem. Note that although there exists a large body of literature on the consequences of frustration within the checkerboard lattice with a *single* atomic orbital per site,[16–23] we are unaware of similar calculations on the present model which deals with doubly degenerate orbitals at each site. An important property of orbitally driven Peierls order in these materials is that the OO leads to Peierls order in *several different crystal lattice directions*.[13] In order to incorporate orbital degeneracy, frustration, and the possibility of Peierls order in multiple directions we consider the following Hamiltonian for a checkerboard lattice with doubly degenerate metal orbitals at each lattice site.

$$H = H_{\mathrm{SSH}} + H_{\mathrm{OO}} + H_{\mathrm{e\text{-}e}}, \tag{1}$$

$$H_{\mathrm{SSH}} = \sum_{i,\mathbf{a},\gamma,\gamma'} t^{\mathbf{a}}_{\gamma\gamma'}(1+\alpha_{\mathbf{a}}\Delta_{i,i+\mathbf{a}})(d^{\dagger}_{i\gamma\sigma}d_{i+\mathbf{a}\gamma'\sigma} + \mathrm{H.c.}) + \frac{1}{2}\sum_{i\mathbf{a}} K_{\mathrm{SSH}}\Delta^2_{i,i+\mathbf{a}}, \tag{2}$$

$$H_{\mathrm{OO}} = \frac{g}{2}\sum_{i,\gamma\neq\gamma'} Q_i(n_{i\gamma'} - n_{i\gamma}) + \frac{1}{2}K_{\mathrm{OO}}\sum_i Q_i^2, \tag{3}$$

$$H_{\mathrm{e\text{-}e}} = U\sum_{i,\gamma} n_{i\gamma\uparrow}n_{i\gamma\downarrow} + \frac{U'}{2}\sum_{i,\gamma\neq\gamma'} n_{i\gamma}n_{i\gamma'}. \tag{4}$$

The Hamiltonian in Eq. (1) consists of, (i) H_{SSH} that contains the kinetic energy and the interion electron-phonon (e-p) coupling [Eq. (2)], (ii) an OO term H_{OO} [Eq. (3)], and (iii) e-e interaction $H_{\mathrm{e\text{-}e}}$ [Eq. (4)] that includes short-range e-e interactions within each site. We describe each of these terms separately below.

H_{SSH} includes electron hopping between same as well as different orbitals. In Eq. (2), $d^{\dagger}_{i\gamma\sigma}$ creates an electron of spin σ in the orbital γ of atom i. γ and γ' correspond to d_{xz} and d_{yz} orbitals, which have lobes that are oriented perpendicular to each other at each site as shown in Fig. 1. The interorbital and intraorbital hopping matrix elements $t^{\mathbf{a}}_{i\gamma\gamma'}$ are based on Slater-Koster parametrization of hopping integrals connecting t_{2g} orbitals.[24] a denotes a unit vector along the x, y, $x+y$, or $y-x$ directions. Each bond indicated in Fig. 1 connects two orbitals at each metal ion site with two orbitals at another site, and is hence written as a 2×2 matrix

$$\begin{pmatrix} t_{xz,xz} & t_{xz,yz} \\ t_{yz,xz} & t_{yz,yz} \end{pmatrix}_{y-x} = \begin{pmatrix} -\frac{1}{2} & -\frac{1}{2} \\ -\frac{1}{2} & -\frac{1}{2} \end{pmatrix}, \tag{5}$$

$$\begin{pmatrix} t_{xz,xz} & t_{xz,yz} \\ t_{yz,xz} & t_{yz,yz} \end{pmatrix}_{x+y} = \begin{pmatrix} -\frac{1}{2} & \frac{1}{2} \\ \frac{1}{2} & -\frac{1}{2} \end{pmatrix}, \tag{6}$$

$$\begin{pmatrix} t_{xz,xz} & t_{xz,yz} \\ t_{yz,xz} & t_{yz,yz} \end{pmatrix}_{x} = \begin{pmatrix} -1 & 0 \\ 0 & 0 \end{pmatrix}, \tag{7}$$

$$\begin{pmatrix} t_{xz,xz} & t_{xz,yz} \\ t_{yz,xz} & t_{yz,yz} \end{pmatrix}_{y} = \begin{pmatrix} 0 & 0 \\ 0 & -1 \end{pmatrix}. \tag{8}$$

All hopping integrals are in units of the $(dd\pi)$ matrix element (set to -1) involving the two d orbitals of the metal atoms and mediated by the p orbital of the anion (not shown explicitly in the figure) in between. In the above, the small $dd\delta$ hoppings have been neglected. Note that electron hoppings along the x (y) direction involve only the d_{xz} (d_{yz}) orbitals. Thus the π bonding among the orbitals, as opposed

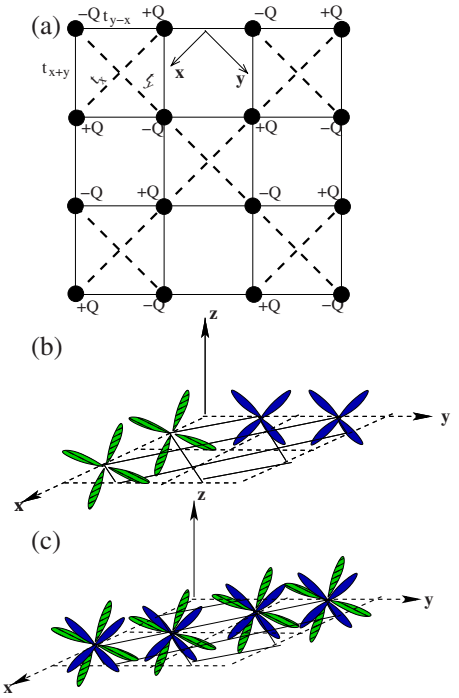

FIG. 1. (Color online) (a) 2D checkerboard lattice with orbital-ordering pattern given by the H_{OO} term in Eq. (3). Filled dots denote metal atom positions, with two orbitals per atom, xz and yz. Hopping terms are included along x, y, $x+y$, and $y-x$ directions as defined in Eqs. (5)–(8). Hopping along the t_x and t_y directions, indicated by dashed lines, is modulated by the interatomic e-p coupling. (b) The $(dd\pi)$ overlap of xz, shown in green (light gray), and yz, shown in blue (dark gray), along the x and y directions. Note that along these directions, nonzero hopping matrix elements exist only along x ($xz-xz$) or y ($yz-yz$) direction. (c) The $(dd\pi)$ overlap of xz and yz orbitals along the $y-x$ direction. The overlap along $x+y$ is similar apart from a change of sign for the interorbital terms.

to the σ bonding in spinels, does not preclude the orbitally induced effective one-dimensionalization.[25]

The interion e-p coupling in H_{SSH} is written in the usual Su-Schrieffer-Heeger (SSH) form.[26] Here $\alpha_{\mathbf{a}}$ is the e-p coupling constant corresponding to the bond between atoms at i and $i+\mathbf{a}$, $\Delta_{i,i+\mathbf{a}}$ the deviation of this bond from its equilibrium length, and K_{SSH} the corresponding spring constant. We include nonzero e-p couplings only along the x and y directions, in keeping with the Peierls distortions in $CuIr_2S_4$ and $MgTi_2O_4$ involving only orbitals of the same kind, and assume e-p couplings of equal strength ($\alpha_x=\alpha_y=\alpha$). We take all spring constants $K_{\mathrm{SSH}}=1$.

The OO term H_{OO} breaks the orbital degeneracy between the two orbitals at each individual site. $n_{i\gamma\sigma}=d^{\dagger}_{i\gamma\sigma}d_{i\gamma\sigma}$ is the number of electrons of spin σ on orbital γ of site i, and $n_{i\gamma}=n_{i\gamma\uparrow}+n_{i\gamma\downarrow}$. The coordinate Q_i couples to the charge density difference between the two orbitals on the site, with a corresponding coupling constant g and spring constant K_{OO}. We fix K_{OO} to the value 1. As written in Eq. (3), the relative phase of the Q_i at each site is unrestricted. Within the model of Ref. 13 the effective one-dimensionalization is a consequence of OO alone and in principle will occur even in the absence of Peierls distortion. We have used this to determine the preferred Q_i mode for both 1 and $\frac{1}{2}$ electron per site by calculating the orbital occupations in several large lattices with open boundary condition (OBC). In a large OBC lattice, the charge densities and bond orders far from the lattice edges spontaneously assume the pattern that would occur in the infinite lattice for 0^+ coupling limit.[27] An alternate approach to determine the dominant OO mode is to calculate in a periodic lattice the energies corresponding to each mode for fixed distortion amplitude; the dominant mode is simply the one with the lowest total energy. In the present case we have performed both sets of calculations for both 1 and $\frac{1}{2}$ electron per site and have determined that the preferred OO mode in both cases is the "checkerboard" pattern of Fig. 1(a), which can be parametrized in terms of a single amplitude $|Q|$ with $Q_i=(-1)^{i_x+i_y}|Q|$, where i_x and i_y are the x and y coordinates of the ith atom.

The third term in the Hamiltonian, $H_{\text{e-e}}$ [Eq. (4)], includes short-ranged Coulomb repulsions. U (U') is the on-atom Coulomb repulsion for electrons in same (different) orbitals. While exact diagonalization has been used successfully for many 1D, quasi-1D, and two-dimensional (2D) lattices involving both e-e and e-p interactions, in the present model with two orbitals per metal site the Hilbert space is too large to treat any meaningful size cluster within exact diagonalization. We will therefore consider first the noninteracting ($U=U'=0$) system, and then consider the effect of U and U' within the unrestricted Hartree-Fock (UHF) approximation, with no assumption of the periodicity of the UHF wave function. Specifically, we replace the interaction terms in $H_{\text{e-e}}$ [Eq. (4)] by

$$
\begin{aligned}
U \sum_{i,\gamma,\sigma,\sigma'} & n_{i\gamma\sigma}\langle n_{i\gamma\sigma'}\rangle - U\sum_{i,\gamma}\langle n_{i\gamma\downarrow}\rangle\langle n_{i\gamma\uparrow}\rangle \\
& + \frac{U'}{2}\Bigg[\sum_{i,\gamma\neq\gamma',\sigma,\sigma'}(n_{i\gamma\sigma}(\langle n_{i\gamma'\sigma}\rangle + \langle n_{i\gamma'\sigma'}\rangle) \\
& - (d^{\dagger}_{i\gamma'\sigma}d_{i\gamma\sigma} + \text{H.c.})\langle d^{\dagger}_{i\gamma'\sigma}d_{i\gamma\sigma} + \text{H.c.}\rangle - \langle n_{i\gamma\sigma}\rangle\langle n_{i\gamma'\sigma}\rangle \\
& - \langle n_{i\gamma\sigma}\rangle\langle n_{i\gamma'\sigma'}\rangle + \langle d^{\dagger}_{i\gamma'\sigma}d_{i\gamma\sigma} + \text{H.c.}\rangle^2\Bigg] .
\end{aligned}
$$

$\langle n_{i\gamma\sigma}\rangle$ and $\langle d^{\dagger}_{i\gamma'\sigma}d_{i\gamma\sigma}+\text{H.c.}\rangle$ are obtained using a combination of self-consistency and simulated annealing for finding their ground-state values. The UHF approximation often gives unphysical results for large interaction strengths and we will primarily focus on small U and U'.

We treat the OO and e-p interactions using a standard self-consistent approach derived from the equations

$$
\frac{\partial\langle H\rangle}{\partial Q} = 0 \quad \frac{\partial\langle H\rangle}{\partial\Delta_{i,i+\mathbf{a}}} = 0. \tag{9}
$$

The self-consistency equations derived from Eq. (9) are used iteratively given an initial starting distortion. In the infinite system the OO or the bond distortion would occur for infinitesimally small coupling constants g and α. In finite-size clusters, however, due to the finite-size gaps between successive energy levels, nonzero coupling constants are required before the symmetry-broken state appears. In the following

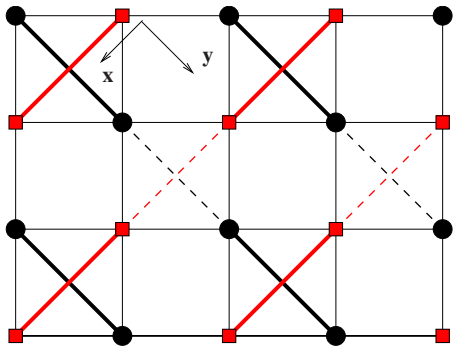

FIG. 2. (Color online) Pattern of the orbital-ordering and bond-order modulation for one electron per atom. Squares (circles) represent atoms with predominant xz (yz) orbital occupation. Bonds alternate in strength along diagonal directions with solid (dashed) lines indicating strong (weak) bonds.

we consider g and α close to the minimum values needed for the broken-symmetry state to occur.

We performed calculations for lattices up to 16×16 (256 atoms with 512 orbitals). The primary difficulty in solving Eq. (9) is that because of the large number of quantities (Q, $\Delta_{i,i+\mathbf{a}}$, and UHF average charge densities) to be determined self-consistently, the calculations often became trapped in local minima before reaching the true ground state. In all cases we have taken care that the true ground state was reached. Below we summarize our numerical results. These are divided into two sections that discuss average charge densities of 1 electron per atom and $\frac{1}{2}$ electrons per atom, respectively.

III. RESULTS

A. 1 electron per atom

The OO term in our model makes the orbital occupancy of the xz and yz orbitals unequal at each site. To measure the degree of OO quantitatively, we calculate the majority charge density $\langle n^+\rangle$, defined as the charge density in the xz orbitals at $+|Q|$ sites [see Fig. 1(a)]. These orbitals form quasi-1D chains in the x direction (sites denoted by squares in Fig. 2). With one electron per site, $\langle n^+\rangle$ ranges from 0.5 to 1, with $\langle n^+\rangle=1$ indicating complete OO, and $\langle n^+\rangle=0.5$ implying the absence of OO. Due to the symmetries present in our model, the quasi-1D chains along x and y directions are identical—the charge density in the yz orbitals at $-|Q|$ sites (denoted by circles in Fig. 2) is also $\langle n^+\rangle$.

As an order parameter for the Peierls distortion, we measure the modulation of the bond order

$$B_{i,i+\mathbf{a},\gamma}=\sum_{\sigma}\langle d^{\dagger}_{i+\mathbf{a},\sigma,\gamma}d_{i,\sigma,\gamma}+\text{H.c.}\rangle. \tag{10}$$

The bond order we are interested in [Eq. (10)] is the expectation value of charge transfer between orbitals of same symmetry belonging to neighboring atoms. The charge transfer is directly coupled to the bond distortion $\Delta_{i,i+\mathbf{a}}$ in Eq. (2) and hence for nonzero $\Delta_{i,i+\mathbf{a}}$ the charge transfer across consecutive bonds shows periodic modulation. The extent of modulation of $B_{i,i+\mathbf{a},\gamma}$ is therefore a direct measure of the SSH distortion strength. As shown in Fig. 2, we find bond-order modulation along x (y) direction to involve xz (yz) orbitals only. The modulation is purely period 2 (dimerization) with alternating strong and weak bonds, and hence we use ΔB, the *difference* between the calculated strong and weak bond orders involving orbitals of a particular symmetry, as the order parameter for the SSH distortion. Because of symmetry, the amplitudes of the bond-order modulations involving the xz orbitals along the x direction, and the yz orbitals along the y directions are identical.

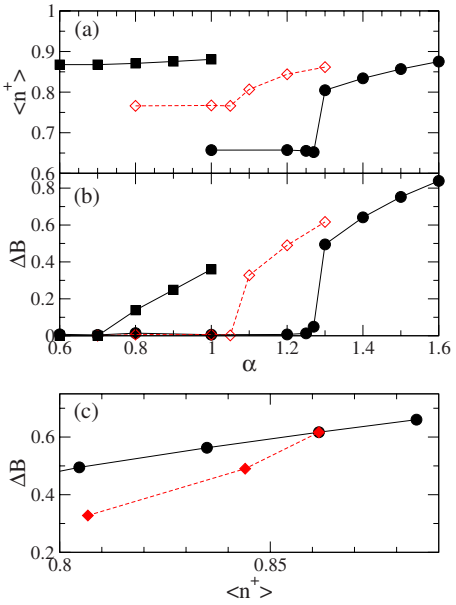

FIG. 3. (Color online) Cooperative orbital-ordering and Peierls bond alternation for one electron per atom, with $U=U'=0$. Calculations are for a 16×16 periodic lattice. (a) Majority charge density (see text) in the orbitals forming the quasi-1D chains following orbital ordering. Here and in (b) circles, diamonds and squares correspond to $g=0.6$, 0.8, and 1.0, respectively. (b) ΔB along the diagonal chain directions (see text and Fig. 2) as a function of α. (c) Bond alternation plotted as a function of charge density. Circles show the effect of increasing g with constant $\alpha=1.3$. Diamonds show effect of increasing α with constant $g=0.8$. Lines are guides to the eye.

As discussed above, whether or not a cooperative orbitally induced Peierls instability occurs for $\langle n^+\rangle<1$, as well as the periodicity of the resultant bond-order wave are both important issues. We first consider the noninteracting limit ($U=U'=0$). The cooperative nature of the OO and bond dimerization is shown in Fig. 3, where we show the results of our self-consistent calculations for 16×16 lattices. As seen in Figs. 3(a) and 3(b), the orbitally induced Peierls state appears only for $\langle n^+\rangle\geq0.8$ with the bond distortion a pure bond dimerization regardless of $\langle n^+\rangle$. As expected for a cooperative transition, $\langle n^+\rangle$ increases with g, as seen in Fig. 3(a). For each g there exists an α_c beyond which there occur simultaneous jumps in $\langle n^+\rangle$ and ΔB (the jump in $\langle n^+\rangle$ becomes progressively smaller as g increases.) The magnitude of α_c decreases with increasing g [see Fig. 3(b)] To further show the cooperative effect, in Fig. 3(c) we show the effects of (i) increasing α at constant g, and (ii) increasing g at constant α.

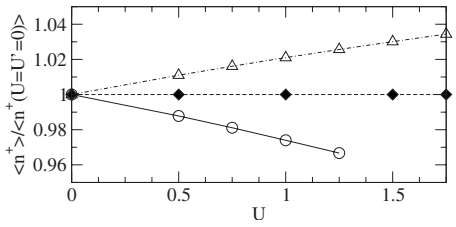

FIG. 4. Majority charge density as a function of U and U' for one electron per atom, normalized with respect to the same quantity for the uncorrelated system. Results shown are for 16×16 periodic lattices with $g=0.8$, $\alpha=1.2$, and $K_{OO}=K_{SSH}=1$. Circles are for $U'=0.3U$, diamonds are for $U'=0.5U$, and triangles are for $U'=0.7U$. Lines are guides to the eye.

While it is to be expected that the orbital order parameter $\langle n^+\rangle$ increases with g, or that the bond alternation parameter increases with α, we find that either of the coupling constants enhances both $\langle n^+\rangle$ and ΔB.

Next we consider the correlated case with nonzero U and U'. As for $U=U'=0$, the orbitally driven Peierls state is again bond dimerized. In Fig. 4 we plot $\langle n^+\rangle$ normalized by its value in the uncorrelated system as a function of U for several values of U'. Within UHF, the combined effect of U and U' can be to either weaken or strengthen the distortion: for fixed U', U tends to weaken the OO and the bond distortion, while for fixed U, U' strengthens both order parameters. Within the UHF approximation for one electron per atom, the effects of U and U' cancel exactly when $U'=\frac{1}{2}U$.

From the Hamiltonian, the consequence of U' is to minimize the intrasite interorbital Coulomb repulsion, which is achieved by orbital ordering. It is thus not surprising that U' has the same effect as g in Fig. 4. The effect of U, as seen in Fig. 4, is however an artifact of the UHF approximation. In the case of the strictly 1D $\frac{1}{2}$-filled band chain with 1 orbital per site, exact diagonalization and quantum Monte Carlo calculations have shown that the Peierls bond alternation is *enhanced* by the Hubbard U.[28] In contrast, the UHF approximation predicts incorrectly that U destroys the bond alternation in the above case.[28] Had we been able to perform exact diagonalization in the present case, we would have found similar enhancement of the bond dimerization by U. This would have had a profound effect on our overall result, reducing significantly the α_c or the threshold $\langle n^+\rangle$ at which the bond dimerization appears.

The most important conclusion that follows from the above is that an orbitally induced Peierls instability can occur even for incomplete OO ($\langle n^+\rangle\sim0.8$), and as long as the instability occurs at all, the bond-order wave is period 2 for $\langle n^+\rangle$ significantly less than 1. Indeed, it is conceivable that the threshold value of $\langle n^+\rangle$ at which the bond dimerization appears can be even smaller than 0.8 for nonzero e-e interactions. We have found no other periodicity or evidence for soliton formation in our calculations. An interesting aspect of the OO driven bond distortion here is the phase relationship between the bond-order wave states involving the d_{xz} and d_{yz} orbitals in Fig. 2. The short bonds along the x and y directions occupy the same plaquettes, yielding a structure that is reminiscent of (but different from) the valence bond crystal obtained within the Heisenberg spin Hamiltonian for the checkerboard lattice.[16] Furthermore, the bond dimerizations along any one direction but on different diagonals of the checkerboard lattice are strictly "in-phase." Both of these indicate that while the bond dimerizations are consequences of effective one-dimensionalization, there exist strong 2D interactions in between both the criss-cross and parallel chains. We ascribe the persistence of the bond dimerization for $\langle n^+\rangle<1$ to the commensurability effect arising from the 2D interactions.

B. $\frac{1}{2}$ electron per atom

In $CuIr_2S_4$ and $MgTi_2O_4$, the distortion along the chain directions is not bond dimerization but a period 4 distortion.[3] This is as expected for a Peierls transition in a 1D chain with carrier density 0.5. We have therefore performed self-consistent calculations within our model Hamiltonian also for density 0.5.

Not surprisingly, we do obtain self-consistently an orbitally ordered state here for nonzero g with $\alpha=0$. Even within an essentially 100% orbitally ordered state (minority orbital charge density $\lesssim0.01$), however, and with very strong α, we were unable to obtain a stable Peierls-distorted state. In all cases our self-consistent simulations converged to states with disordered bond distortions and charge densities, indicating vanishing bond-charge distortion in the thermodynamic limit. We obtained similar results after including U and/or U' within the UHF approximation. We conclude that for electron density away from 1 electron per atom, orbitally driven Peierls ordering does not occur within our model in the noninteracting limit or within the mean-field approach to e-e interactions.

We ascribe the absence of bond-charge distortion here to the important role played by the interaction among the criss-crossing chains within the checkerboard lattice. We have already pointed out in Sec. III A that the stabilization of the perfect period 2 distortion for the case of 1 electron per atom, even in the absence of complete OO, is a signature of such a 2D interaction. Similar 2D interactions should be relevant also for carrier density 0.5. Since within mean-field theory the Peierls instability in 2D is limited to carrier density of 1, the absence of the bond-charge distortion in the present case is to be anticipated. On the other hand, we have recently shown in a series of papers that specifically for this carrier density and 1 orbital per site, nonzero e-e interactions can strongly stabilize bond-charge ordered states in 2D lattices.[27,29] In the case of the checkerboard lattice with a single orbital per site, plaquette spin-singlet formation (though without charge ordering) has similarly been found for the same carrier concentration.[30] It is conceivable that similar effects of e-e interactions persist in the present case with two degenerate orbitals per site.

Unfortunately, performing a realistic calculation with finite U that goes beyond the UHF approximation in the present case is beyond our computational capability. We have therefore investigated our model Hamiltonian (1) in the limit of $U\rightarrow\infty$, where we assume band orbital occupancy corresponding to that for spinless fermions. Figure 5 shows the same order parameters as in Fig. 3 for the spinless fermion

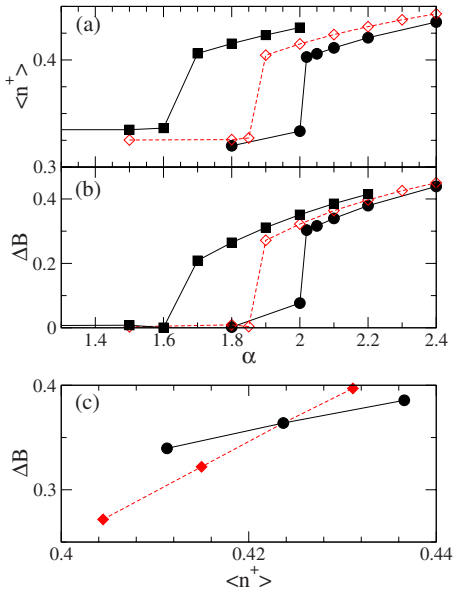

FIG. 5. (Color online) Cooperative orbital-ordering and Peierls bond alternation for 0.5 spinless fermions per atom. Calculations are for a 16×16 periodic lattice. (a) Majority charge density in the orbitals forming the 1D chains. Here and in (b) circles, diamonds and squares correspond to $g=0.6$, 0.8, and 1.0, respectively. (b) ΔB along the diagonal chain directions (see Fig. 2) as a function of α. (c) Bond alternation versus majority charge density. Circles show the effect of increasing g with constant $\alpha=1.3$. Diamonds show effect of increasing α with constant $g=0.8$. Lines are guides to the eye.

case. While the transition occurs here for a slightly larger value of the coupling constant α, it is otherwise identical to the transition with 1 electron per atom, viz., bond dimerization occurs along the diagonal directions, and OO and bond distortion reinforce each other cooperatively.

IV. DISCUSSION

In summary, we have carried out numerical studies on the 2D checkerboard lattice with two degenerate directional orbitals per site—a model system that like the spinel compounds can in principle exhibit Peierls bond distortions and charge ordering in multiple directions. In addition to OO and bond modulation terms, our model Hamiltonian includes both intraorbital and interorbital e-e correlations that were treated within the UHF approximation. Although some of our results have strong implications for the spinels, it is useful to precisely understand the differences between the spinel and checkerboard lattices such that the applicability as well as limitations of our model can both be understood. One difference between the two lattices is that the plaquettes in the 2D checkerboard lattice do not correspond to the tetrahedra in the spinel lattice because of the difference between horizontal and vertical bonds in Fig. 1(a) on the one hand and the diagonal bonds on the other.[16] What is more important in the present context is that the OO in our model is not driven by a band JT transition that destroys the degeneracies of the atomic orbitals in the model of.[13] Within our model the two orbitals of different symmetries on a given atom are both potentially active orbitals.

We believe that our demonstration of the cooperative interaction between OO and the Peierls instability in Sec. III A, where each broken symmetry enhances the other, is of direct relevance to the t_{2g}-based spinel systems, where qualitative discussions have suggested similar results.[13] Similarly, our observation that the period two bond distortion persists for 1 electron per atomic site even for incomplete OO, with majority charge density as low as 0.8 per orbital, may also be of significance for the spinels. This should be particularly true for nonzero onsite Hubbard interaction, which will tend to decrease the amplitude of the OO. Complete OO in the real systems $CuIr_2S_4$ and $MgTi_2O_4$ requires that the energy gap due to the JT distortion is significantly larger than the Hubbard interaction. It is at least equally likely that the commensurate charge and bond distortions found in the experimental systems are not due to complete OO but are consequences of the complex interactions between the crisscrossing chains in the spinel lattice, as in the checkerboard lattice.

The implication of the absence of the Peierls instability for the case of $\frac{1}{2}$ an electron per atom in the checkerboard lattice within one-electron theory is less clear. One possible implication is that our results for the 2D checkerboard lattice are irrelevant for the three-dimensional (3D) spinel lattice because of the fundamental difference between them that has already been pointed out in the above. In $CuIr_2S_4$, the only active orbital following the OO is the d_{xy} orbital,[13] which has been excluded within our model. It is thus conceivable that the 1D character of the active orbitals in $CuIr_2S_4$ following OO is much stronger than in the checkerboard lattice and this is what drives the metal-insulator transition in the real system. It is, however, equally likely that the 3D interactions between the d_{xy}-based chains are as strong as the 2D interactions in the checkerboard lattice (recall, for example, that commensurate periodicity for independent 1D chains requires complete OO, see above). In this case our null result for the uncorrelated checkerboard lattice would imply nonnegligible contribution of e-e interaction to the metal-insulator transitions in $CuIr_2S_4$ and $LiRh_2O_4$. Further theoretical work based on the 3D pyrochlore lattice as well as experimental work that determines the extent of OO in the real systems will both be necessary to completely clarify this issue.

Finally, assuming that e-e interactions play a role, which is subject to further investigations as discussed above, this raises an interesting question, viz., what ultimately is the driving force behind the metal-insulator transitions in $CuIr_2S_4$ and $LiRh_2O_4$? Three of us have argued elsewhere that for carrier concentration precisely 0.5, there is a strong tendency to form a paired-electron crystal (PEC), in which there occur pairs of spin-singlet bonded sites separated by pairs of vacancies.[31] This tendency to spin pairing is driven by nearest-neighbor antiferromagnetic (AFM) correlations (as would exist in a large Hubbard-U system) and is enhanced in the presence of lattice frustration. Although the original calculations are for the anisotropic triangular lattice with a single orbital per site, the same tendency to spin-singlet formation can persist also in the spinel lattice. If the

insulating state in the spinels $CuIr_2S_4$ and $LiRh_2O_4$ can be understood as a PEC with spin-singlet pairing driven by AFM correlations, it may further indicate that e-e interactions play an important role in superconductivity found in several structurally related spinels. Whether or not e-e interactions play a role in the observed superconductivity in the spinels $LiTi_2O_4$, $CuRh_2S_4$, and $CuRh_2Se_4$ has remained a lingering question.[32,33] If the insulating state in this class of materials is indeed a PEC, the superconducting spinels should perhaps be included among the systems in which superconductivity is driven not entirely by BCS electron-phonon coupling.

ACKNOWLEDGMENTS

Work at Mississippi State University and the University of Arizona was supported by the U.S. Department of Energy under Grant No. DE-FG02-06ER46315. Collaboration between the U.S. teams and the S. N. Bose National Centre was supported by a travel grant from the Indo-U.S. Science and Technology Forum under Grant No. JC/54/2007/"Correlated electrons in materials." The authors gratefully acknowledge discussion with D. D. Sarma. S.S. thanks CSIR for financial support.

[1] Y. Tokura and N. Nagaosa, Science **288**, 462 (2000).
[2] E. Dagotto, Science **309**, 257 (2005).
[3] P. G. Radaelli, New J. Phys. **7**, 53 (2005).
[4] H. Tsunetsugu and Y. Motome, Phys. Rev. B **68**, 060405 (2003).
[5] Y. Motome and H. Tsunetsugu, Prog. Theor. Phys. **160**, 203 (2005).
[6] S. Sarkar, T. Maitra, R. Valenti, and T. Saha-Dasgupta, Phys. Rev. Lett. **102**, 216405 (2009).
[7] N. Nishiguchi and M. Onoda, J. Phys.: Condens. Matter **14**, L551 (2002).
[8] K. Matsuno, T. Katsufuji, S. Mori, Y. Moritomo, A. Machida, E. Nishibon, M. Takata, M. Sakata, N. Yamamoto, and H. Takagi, J. Phys. Soc. Jpn. **70**, 1456 (2001).
[9] M. Schmidt, W. Ratcliff II, P. G. Radaelli, K. Refson, N. M. Harrison, and S. W. Cheong, Phys. Rev. Lett. **92**, 056402 (2004).
[10] P. G. Radaelli, Y. Horibe, M. Gutmann, H. Ishibashi, C. H. Chen, R. M. Ibberson, Y. Koyama, Y. S. Hor, V. Kiryukhin, and S. Cheong, Nature (London) **416**, 155 (2002).
[11] Y. Okamoto, S. Niitaka, M. Uchida, T. Waki, M. Takigawa, Y. Nakatsu, A. Sekiyama, S. Suga, R. Arita, and H. Takagi, Phys. Rev. Lett. **101**, 086404 (2008).
[12] J. D. Dunitz and L. E. Orgel, J. Phys. Chem. Solids **3**, 20 (1957).
[13] D. I. Khomskii and T. Mizokawa, Phys. Rev. Lett. **94**, 156402 (2005).
[14] M. Isobe and Y. Ueda, J. Phys. Soc. Jpn. **71**, 1848 (2002).
[15] S. Mazumdar, S. N. Dixit, and A. N. Bloch, Phys. Rev. B **30**, 4842 (1984).
[16] J.-B. Fouet, M. Mambrini, P. Sindzingre, and C. Lhuillier, Phys. Rev. B **67**, 054411 (2003).
[17] O. Tchernyshyov, O. A. Starykh, R. Moessner, and A. G. Abanov, Phys. Rev. B **68**, 144422 (2003).
[18] E. Runge and P. Fulde, Phys. Rev. B **70**, 245113 (2004).
[19] O. A. Starykh, A. Furusaki, and L. Balents, Phys. Rev. B **72**, 094416 (2005).
[20] D. Poilblanc, K. Penc, and N. Shannon, Phys. Rev. B **75**, 220503 (2007).
[21] F. Trousselet, D. Poilblanc, and R. Moessner, Phys. Rev. B **78**, 195101 (2008).
[22] T. Yoshioka, A. Koga, and N. Kawakami, J. Phys. Soc. Jpn. **77**, 104702 (2008).
[23] T. Yoshioka, A. Koga, and N. Kawakami, Phys. Rev. B **78**, 165113 (2008).
[24] W. A. Harrison, *Electronic Structure and the Properties of Solids* (Freeman, New York, 1980).
[25] We have confirmed this by performing the same calculations with degenerate p_x and p_y orbitals in which case the bonding along the chain directions is σ.
[26] W. P. Su, J. R. Schrieffer, and A. J. Heeger, Phys. Rev. B **22**, 2099 (1980).
[27] S. Mazumdar, R. T. Clay, and D. K. Campbell, Phys. Rev. B **62**, 13400 (2000).
[28] D. Baeriswyl, D. K. Campbell, and S. Mazumdar, in *Conjugated Conducting Polymers*, edited by H. Kiess (Springer-Verlag, Berlin, 1992), pp. 7–133.
[29] R. T. Clay, S. Mazumdar, and D. K. Campbell, J. Phys. Soc. Jpn. **71**, 1816 (2002).
[30] M. Indergand, C. Honerkamp, A. Läuchli, D. Poilblanc, and M. Sigrist, Phys. Rev. B **75**, 045105 (2007).
[31] H. Li, R. T. Clay, and S. Mazumdar, J. Phys.: Condens. Matter **22**, 272201 (2010).
[32] P. W. Anderson, G. Baskaran, Z. Zou, and T. Hsu, Phys. Rev. Lett. **58**, 2790 (1987).
[33] W. E. Pickett, Rev. Mod. Phys. **61**, 433 (1989).